Proceedings of the Estonian Academy of Sciences
2025, **74**, 2S, 312–321

https://doi.org/10.3176/proc.2025.2S.06

www.eap.ee/proceedings
Estonian Academy Publishers

MEASUREMENT ELECTRONICS

RESEARCH ARTICLE

Received 16 December 2024
Accepted 2 April 2025
Available online 5 June 2025

Keywords:
eddy current, defects, surface, metals

Corresponding author:
Olev Märtens
olev.martens@taltech.ee

Citation:
Märtens, O., Land, R., Metshein, M., Abdullayev, A., Vennikas, H., Le Moullec, Y. et al. 2025. Detection of surface defects in metals: a case study. *Proceedings of the Estonian Academy of Sciences*, **74**(2S), 312–321.
https://doi.org/10.3176/proc.2025.2S.06

Detection of surface defects in metals: a case study

Olev Märtens[a], Raul Land[a], Margus Metshein[a], Anar Abdullayev[a], Henri Vennikas[a,b], Yannick Le Moullec[a] and Marek Rist[a]

[a] Thomas Johann Seebeck Department of Electronics, Tallinn University of Technology (TalTech), Ehitajate tee 5, 19086 Tallinn, Estonia

[b] Institute of Technology, TTK University of Applied Sciences, Pärnu mnt 62, 10135 Tallinn, Estonia

ABSTRACT

Several approaches can be used to find defects in metal surfaces. Eddy current testing is a simple and efficient method for non-destructive testing of metals, identifying alloys, measuring coating thickness, and detecting corrosion. Impedance spectroscopy enables depth profiling and high-speed measurements in real-time manufacturing. For example, in the wood processing industry, early detection of cracks in high-speed band saws is crucial. Electromagnetic testing, particularly eddy-current-based methods, is widely used. This paper reviews existing solutions and investigates cracked saw blade specimens using planar coils in the 100 kHz–10 MHz range. Results show that higher frequencies improve crack detection. Future research should focus on high-speed detection and machine vision-based solutions.

1. Introduction

This paper is an extended version of the conference paper presented at the Baltic Electronics Conference 2024 – Märtens et al., "Detection of cracks in a sawblade by eddy current measurements" [1].

Several methods can be used to detect defects in metals, alloys, coatings, and metal structures. Visual inspection – nowadays often implemented as automatic optical inspection (AOI) and combined with machine learning (ML) algorithms – is a powerful and universal approach and should always be considered when applicable [2]. If the object under test (OuT) is not directly visible (e.g., a steel plate beneath a layer of paint), X-ray imaging can be used, although this solution is typically costly and inconvenient. A highly efficient, contactless method for non-destructive testing (NDT) of metal structures and properties, including surface layers, is eddy-current testing (ECT) [3,4], which is described in more detail below.

While the remainder of Section 1 gives an overview of eddy current measurement and other inspection methods, Section 2 presents a case study of saw blade testing that advances the state of the art through a model-based approach.

1.1. Eddy current measurements

Eddy current (EC), also known as magnetic induction, measurements have been used for NDT of metal materials and structures, e.g., in the field of aerospace, for several decades. Typical tests include comparing various parts of the structure or specimen under test with known (reference) pieces, by analyzing the differences in their electromagnetic signatures.

The EC phenomenon is explained in Fig. 1, where a primary alternating magnetic field arising from the excitation by the sensor coil causes a secondary alternating magnetic field in the electrically conductive sample, thereby generating ECs (Fig. 1).

In the simplest case [6], the measurement can be performed using a measurement probe in the form of a single inductive coil positioned above the material under test (e.g., a metal plate), as shown in Fig. 2. The electrical impedance (both real and imaginary components) depends on the electrical and magnetic properties of the OuT [7,8] – specifically, its magnetic permeability (μ) and electric conductivity (σ). Impedance is also influenced by the measurement frequency (f) and thickness (t) of the measured object, such as a metal plate.

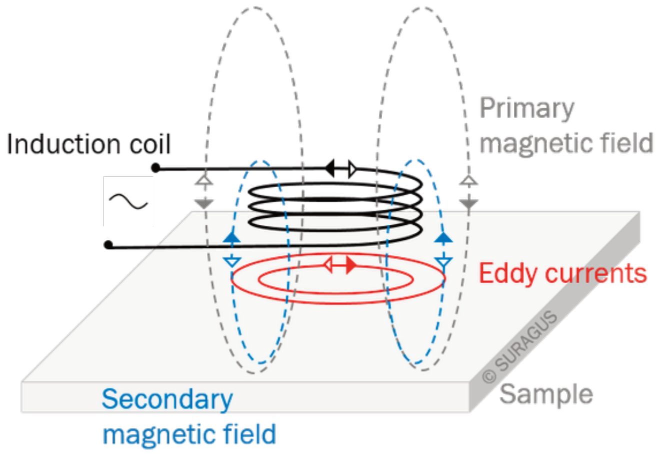

Fig. 1. Eddy current phenomenon [5].

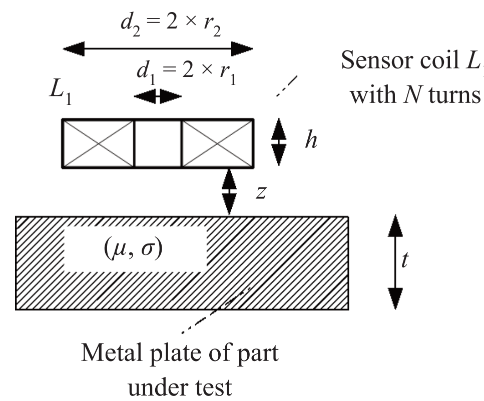

Fig. 2. Eddy current measurement of metals.

Moreover, the results depend on the geometry of the measurement coil – specifically, the inner and outer radiuses (r_1 and r_2) and height (h). Furthermore, the sensor liftoff – the air gap (z) between the sensor coil and the OuT – also plays an important role.

It is important to note that the penetration depth of the EC measurement depends on the measurement frequency and the magnetic and electrical properties of the OuT, as given by Eq. 1 [6]:

$$\delta = 1/\sqrt{(\pi f \mu \sigma)}. \tag{1}$$

According to this equation, low frequencies penetrate deeply into the OuT, while higher frequencies measure only the near-surface properties of the OuT. Thus, acquiring the impedance spectrum of the sensor coil over a wider frequency range allows for characterization of the depth profile of the OuT beneath the probe. By scanning the sensor probe, the 3D properties of the OuT can be acquired.

Already since the 1960s, the analytical Dodd–Deeds model has existed for forward and inverse modeling of electromagnetic properties (electrical conductivity and magnetic permeability), describing a setup with a measurement coil positioned above metal plates or inside/outside metal tubes to be characterized [9]. Moreover, since the 1980s, analytical models for measurement setups with two separate transmit and receive coils have also been available [10,11]. Furthermore, it is worth mentioning that multilayer [12] and even continuous depth profiles of the OuT can be solved analytically [13] using a similar approach.

1.2. Works conducted in the field of ECT at TalTech

The model-based approach used at TalTech enables metrologically accurate measurements without the need for calibration against standard specimens with known properties.

- Under contract with the European Anti-Fraud Office (OLAF), the project "Study of the Euro Coin conductivity calibration procedure for obtaining certified reference standards (2007–2009)" aimed to improve eddy current measurement accuracy and build a metrological traceability chain. This work was carried out in cooperation with Metrosert (Estonia) and other partners. One aspect of the R & D was the correction of inhomogeneities of the OuT [14].
- In the EU FP7-SME project VFP494 "SafeMetal" (2010–2012), the main focus was the development of improved eddy current coin measurement and validation solutions. Several prototypes were developed, including a low-cost, fast DSP-based model (Fig. 3, [15]). A multifrequency

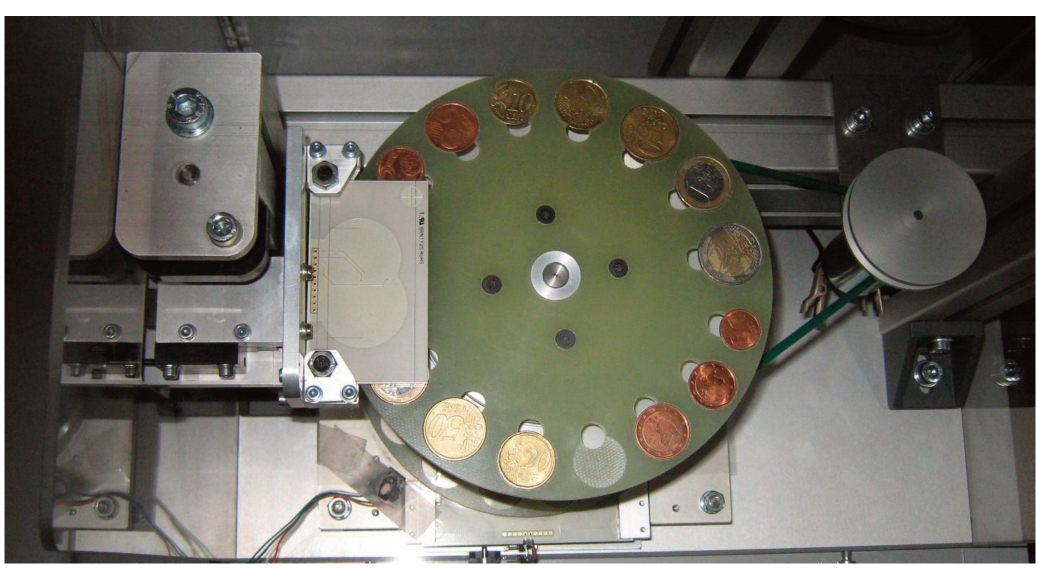

Fig. 3. Testbench 2 for coin validation R & D [15].

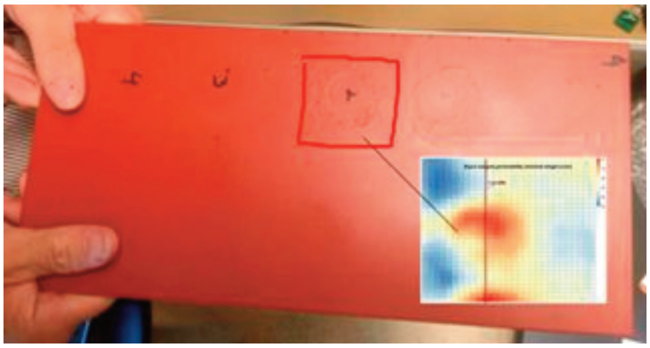

Fig. 4. Painted specimen with rust [22].

measurement approach proved beneficial (e.g., as proposed in [16]), particularly because coins such as 1€ and 2€ are multilayer objects. Patented solutions developed at TalTech, including several implementation variants [17], are efficient for coin validation and other ECT applications. For instance, one solution [18] enables acquiring 1000 spectra per second, allowing for extremely high-speed measurements. Some aspects of measurement accuracy are discussed in [19,20].

- Industrial project with Autoliv company. In the contract Lep17094 "Preliminary study of measurement techniques" (2017–2021), a solution for the automotive industry was developed for high-speed and accurate testing of the quality of mechanically and thermally processed steel components. The challenge lies in obtaining highly precise measurements at high speed (e.g., 100 measurements of full impedance spectra per second) [21].
- Measurement of steel corrosion. A feasibility study was carried out for the Estonian Innovation Institute (EII, at that time a company of UK-based PERA-organization). It was shown that EC impedance spectroscopy can effectively identify and measure the depth and size of corrosion areas on the surface of steel, even under paint. The key idea here [23] is that the corroded part (rust) has much lower electrical conductivity and magnetic permeability compared with the original steel material. The performed work is described in [22] (see also Fig. 4).
- Differentiation of various steel grades. There has been some industrial interest in distinguishing various steel grades. For example, when comparing AISI1201 with AISI1304, the estimated conductivity is clearly distinguishable. The background of this interest lies in the fact that manufacturers of home kitchen, bathroom, and similar appliances often use cheaper materials than claimed.
- Other works. A recent work, performed in co-operation with TalTech material engineering scientists, focused on EC-based R & D of welded joints of cermets to steel and is described in [24].

1.3. Other inspection methods

For industrial applications, NDT methods are preferred for online quality testing of products and for inspecting machinery to enable advanced quality monitoring, diagnostics, and maintenance.

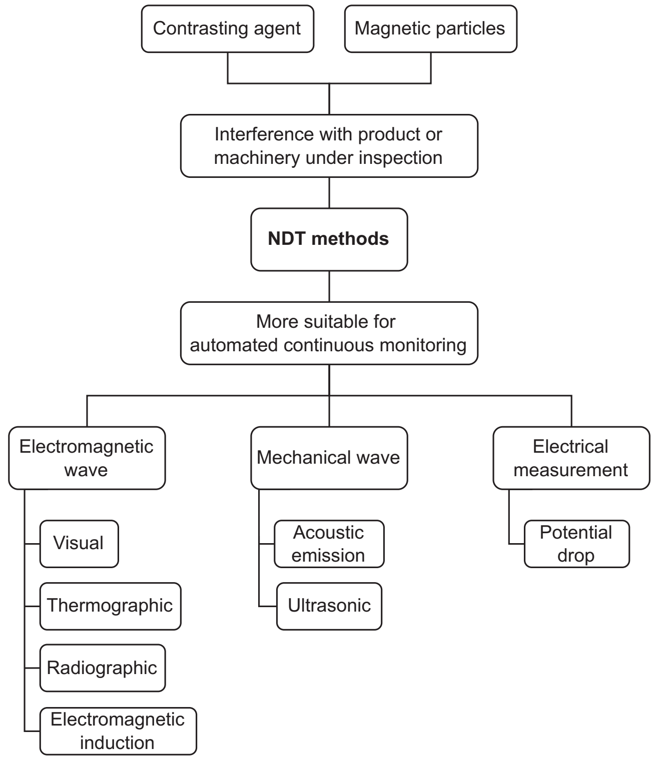

Fig. 5. Non-destructive testing methods suitable for continuous online monitoring.

Some NDT methods require extra processing steps and are therefore less suitable for online testing. For example, such methods include adding contrasting agents or magnetic particles to a surface to detect microscopic features that remain hidden to normal visual inspection.

A more suitable subset of NDT methods for online inspection is shown in the bottom half of Fig. 5. These methods employ sensors that do not require additional tampering with the subject under inspection, allowing for continuous online product or machinery monitoring without noticeable disruption to production processes or the object itself [25–27].

While the current paper focuses on (possibly high-speed) ECT testing, vision-based solutions may significantly complement ECT testing in the near future.

Various approaches to hairline crack detection exist; morphological operations can be applied independently or in combination with convolutional neural networks (CNNs).

In [28], a digital image correlation approach is proposed, where images of the loaded and unloaded structure surfaces are cross-correlated for crack detection, providing displacement and strain fields.

In [29], successive contour estimation is used to establish a morphological operations pipeline consisting of denoising, segmentation, and mapping to preserve accurate contour information of the subject under inspection while suppressing other image features, enabling defect detection through contour estimation.

An iterative thresholding technique applies image binarization thresholds in successive iterations to extract defect information from color images of metal surfaces [30].

Using a CNN (VGG16), it is possible to accurately locate and measure cracks in metal surfaces by identifying regions of interest and then applying morphological operations [31].

Another CNN (HRNet)-based approach emphasizes semantic segmentation as a possible solution to addressing challenges such as low contrast between defects and background, weak boundary definition, and an imbalanced distribution of defect types within images [32].

Automated visual inspection is usually performed using digital imaging devices, which enable image processing to enhance and detect surface features of interest. Visual inspection can be arranged to check the input quality of materials for different processes (e.g., quality classification of fruits and vegetables or animal hides [33]) or the output of production processes (e.g., industrial production [34], such as textile industry [35] or steel industry [36]), as well as for inspections related to maintenance and diagnostics (e.g., inspection of infrastructure [37], such as concrete bridges and buildings).

Various signal processing methods are used to reveal surface and subsurface defects from thermographic images. The usual setup consists of a heat source and an infrared (IR) camera. After a short period of heating the surface, heat signature images are captured and processed according to the selected algorithm. Many different types of defects can be revealed, including different types of cracks, structural damage incoherences, and corrosion [38].

At the higher frequency (or shorter wavelength) end of the electromagnetic spectrum, the X-ray and γ-ray regions are used in NDT for imaging subjects under test to identify internal features of interest (cracks, voids, structural incoherences). Moreover, X-ray methods can reveal material properties, crystallographic structure, and residual stress, while X-ray computed tomography is used to reconstruct a three-dimensional representation of the subject under inspection [25,27].

Passive acoustic emissions (AE) can emerge from the substrate under stress as it possesses defects such as cracks, fractures, or delamination. The frequency of the emitted signal can vary between 10 kHz–1 MHz. Either piezoelectric sensors, fiber-optic sensors, or micro-electromechanical sensors (MEMS) are used to detect the acoustic signals [39].

Ultrasonic frequencies in the range of 0.5–25 MHz of the mechanical (sound) wave are used for measuring hidden subsurface features such as defects, cracks, delamination, and uneven thickness. The ultrasonic transducers can be configured as a single point of contact or, as in RADAR applications, in a phased array. It is also possible to employ contactless ultrasonic testing, where lasers are used to induce and measure ultrasonic backscatter, though this application is mainly confined to thin sheet materials [25,27]. Interesting research in ultrasonic NDT has also been performed at the INSA Centre Val de Loire, France (see, e.g., [40]).

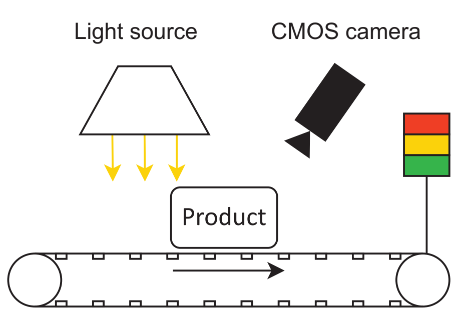

Fig. 6. An example layout of industrial visual inspection.

It is possible to apply either AC or DC current across the surface of the substrate and measure the voltage drop accordingly. Surface flaws, such as cracks, are characterized by a change in the voltage drop [25].

2. Case study: saw blade testing

Wood processing in industry includes several processes. One of these is wood cutting, performed by band saws at high speeds – often exceeding 50 m/s. There is a need for early warning systems to detect crack formation, which typically begins near the saw teeth and is initially small in size (submillimeter in width). A key challenge is also the required testing speed, as tens of thousands of saw teeth may need to be tested per second. Therefore, the actual speed of measurements – for example, using eddy current testing – needs to exceed 100 000 measurements per second. Unfortunately, existing solutions are limited by several orders of magnitude in terms of measurement speed [41,42].

Although other methods exist, such as monitoring AEs during operation, or measuring vibration and tension of the cutting tools, the most common approach is electromagnetic (e.g., EC-based) testing.

The motivation for the performed experimental research stems from the lack of publicly available sensor data on electromagnetic testing of real-life industrial saw blades used in the wood-processing industry.

2.1. Known solutions for saw blade crack detection

An example of a commercial test system is the band saw monitoring system by the USNR company [43]. Inductive sensors are used to control the work of the saw band. The system claims to enable the "detection of cracks in the saw bands at an early stage," but a detailed description of the accuracy and speed limitations is not publicly available.

Another example is provided by the Foerster Group, a company specializing in ECT solutions [41], which offers the EC-based testing "Statograph" solution for testing saw bands. It is claimed that "under optimal conditions, defect resolutions of up to 30 µm are possible." Measurement frequencies can be selected from 1 kHz, 3 kHz, 10 kHz, 30 kHz, 100 kHz, 300 kHz, 1 MHz, 3 MHz, or 10 MHz.

Although the measurement speed is not disclosed in the technical data [42], it is probably limited to only a few tens of measurements per second.

The way the cracks start and grow is characterized in the PhD thesis [44]. Various approaches for detecting cracks in saw blades have been described in the literature:

- Vibration and tension testing. Combined monitoring of blade vibration and tension sensor data has been used to estimate crack length [45].
- AE-based measurements. AE signals have been used to detect possible defects during the cutting process [46], including sensor-data fusion of various AE signals [47].
- EC measurement-based testing is already described in general terms in the introduction. In addition, the review on ECT [48] published in 1999 covers both forward and inverse modeling and includes also time-domain analysis, e.g., for pulsed-signal-based testing. Some mathematical solutions for pulsed ECT (PECT) are given in [49–53]. A recent (2022) paper focuses on EC measurements for planar structures [54]. The latest review (2023) addresses "conventional and advanced non-destructive testing techniques for detection and characterization of small-scale defects" [55]. Determining crack depth by ECT is discussed in [56].
- Alternating current field measurement (ACFM), a method similar to ECT, investigates surface discontinuities using either a single sensor or a sensor array [57,58].
- Giant magnetoresistive (GMR) sensors have also shown promise for capturing ECT response signals with very high spatial resolution [59].

The authors' experience in ECT includes measurement of the hardness of steel details [60].

3. Experimental setup and results

3.1. Example test piece to be investigated

A fragment of a band saw blade with a couple of small cracks, previously used in a wood processing industrial company, has been investigated in the current work (Fig. 7).

The cracks on the surface are hardly visible in the original saw blade image (Fig. 8a), but they become much more clearly identifiable after modifying the brightness, contrast, and especially the gamma correction of the image (Fig. 8b).

3.2. Sensor coils used

The measurement (sensor) printed circuit board (PCB, i.e., planar) coils used in our ECT measurement setup are from the Texas Instruments LDC Reference Coils set [61]. The smaller-size circular coils, labeled as N, O, Q, P, R, and S, were initially considered for the experiments (see Table 1).

As described in the previous conference paper [1], experiments were performed with coils N, O, P, and S. Figure 9 shows the O, P, and S PCB coils. The acquired resulting plots were presented in the same paper.

(a)

Default (original) image

(b)

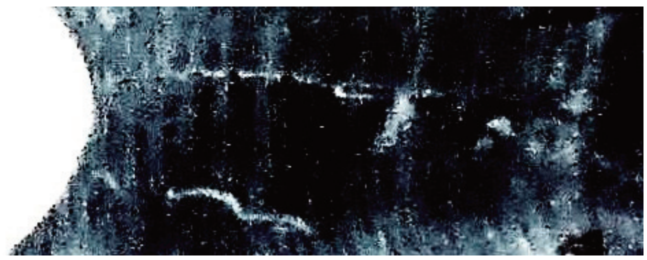

Enhanced image

Fig. 8. Default (a) and enhanced (b) image of the saw blade surface.

Table 1. Coils considered for measurement. Coils N, O, P, and S were selected for conducting the measurements

Coil type	Parameters			
	Dimensions, mm	Turns × layers	L, μH	R, Ω
N	d = 3	3 × 4	0.25	0.6
O	d = 8	11 × 4	8.70	4.7
P	d = 5	9 × 4	2.85	2.3
Q	d = 6	9 × 4	4.82	3.3
R	d = 4	6 × 4	1.09	1.4
S	d = 10	16 × 2	22.00	6.0

Fig. 7. Fragment of the band saw.

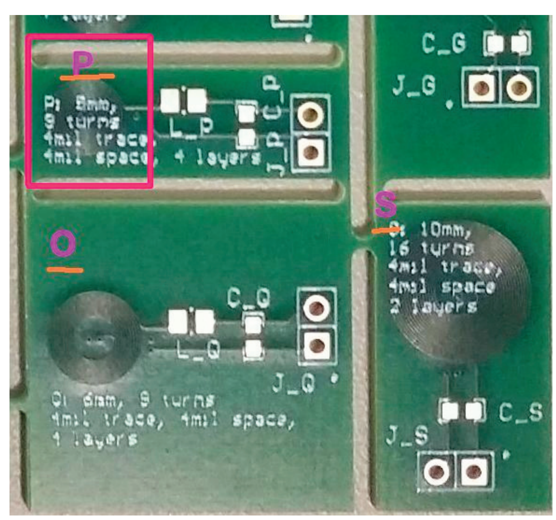

Fig. 9. Images of selected measurement coils – O, P, and S [61].

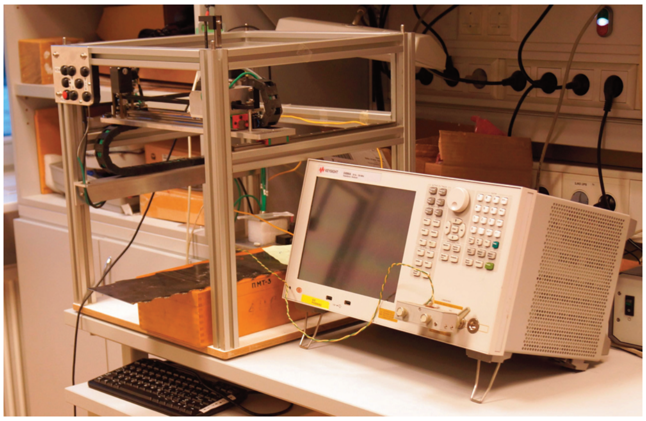

Fig. 10. Measurement setup. Left: Keysight impedance analyzer E4990A. Right: a self-made mechanical 3D scanner that moves the planar sensor coil above the surface of the piece of saw blade under test (laid on the orange wooden box).

In the current paper, the results obtained with coil P are shown and further investigated, as they demonstrated the most appropriate sensitivity for our purpose.

3.3. Measurement setup and procedure

The ECT test setup includes a Keysight impedance analyzer E4990A and a self-made 3D scanner (Fig. 10), which moves the planar sensor coil above the surface of the OuT (the piece of saw blade laid on the orange wooden box). The scan was performed in the region around the crack, with three liftoffs (air gaps) – 0.1, 0.5, and 1.0 mm –, across a wide frequency range from 1 kHz to 100 MHz.

3.4. Results of EC measurements

Based on earlier work [1], the results obtained using coil P at relatively high frequencies (in the range of 5 to 10 MHz) were selected for future work, aiming to implement the next prototype demonstrator.

At such frequencies, the penetration depth of the electromagnetic field allows us to clearly detect the defects on the surface of the saw blade, while the measurement frequencies are feasible at reasonable cost and accuracy.

In Fig. 11a, the variation of both the real and imaginary (inductive) parts of the sensor coil impedance (Ω) at a frequency of about 7.7 MHz (selected as representative in the middle of the reasonable range of 5–10 MHz) is shown, while scanning across the crack. As seen in the plot, the crack is well distinguishable at liftoffs (air gaps) of 0.1 and 0.5 mm, especially through the imaginary component of the impedance. This confirms that the proposed solution is capable of detecting such defects. However, the measurement results significantly depend on the liftoff of the sensor coil. Notably, as will be described further, the real and imaginary components of the sensor coil impedance change in opposite directions, which makes it possible to correct for the influence of liftoff.

The initial value of the coil impedance is about 10 Ω for the real component and 140 Ω for the imaginary component.

In Fig. 11b, the variation in both real and imaginary (inductive) parts of the sensor coil impedance at a frequency

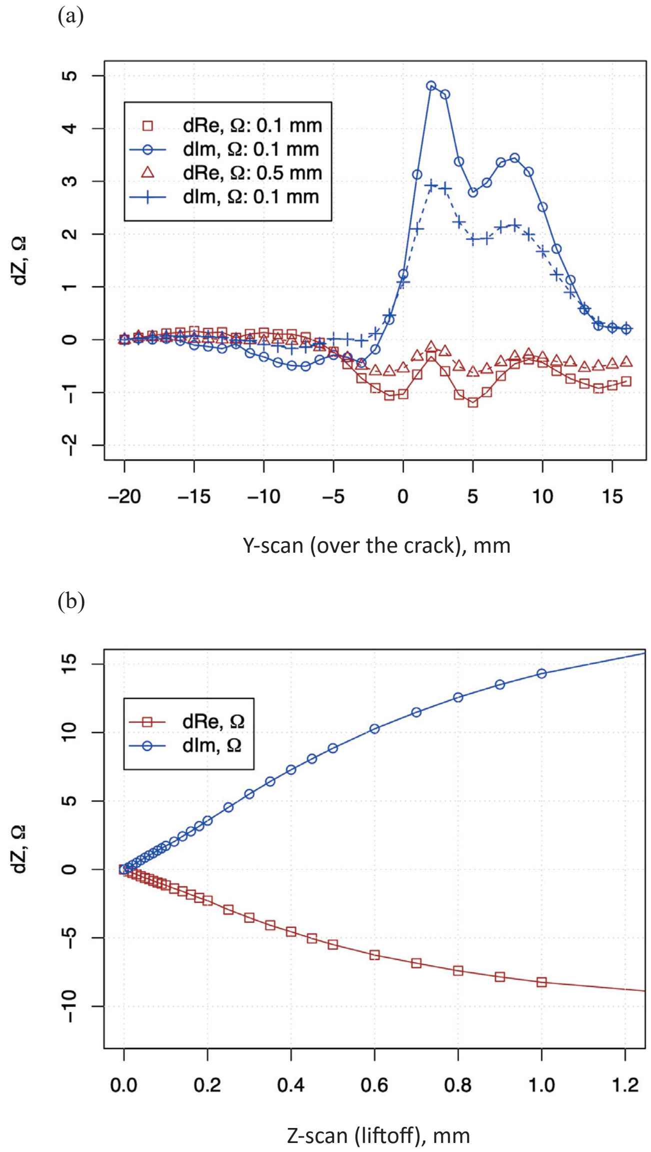

Fig. 11. Y-scan over the crack (a) and Z-scan (liftoff) scan (b) results.

of about 7.7 MHz is shown, while scanning the dependency on the liftoff. As seen in the plot, sensor coil impedance is strongly dependent on the liftoff value, in both the real and imaginary components. From this plot and curves, it can also be estimated that a change in liftoff, around small values, results in a change of $-11.5 + 17.2i$ complex Ω per mm liftoff for this specific frequency and specimen.

From this linear approximation dependency, the liftoff can be estimated from the Y-scan. The result is shown in Fig. 12.

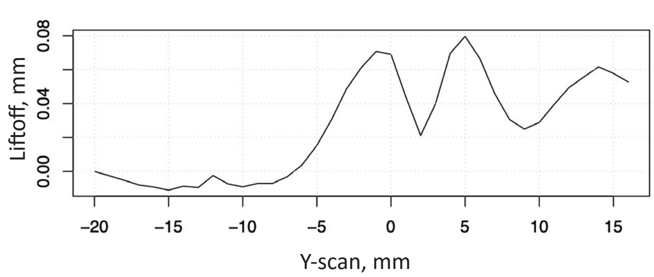

Fig. 12. Liftoff estimation from the Y-scan.

(a) (b)

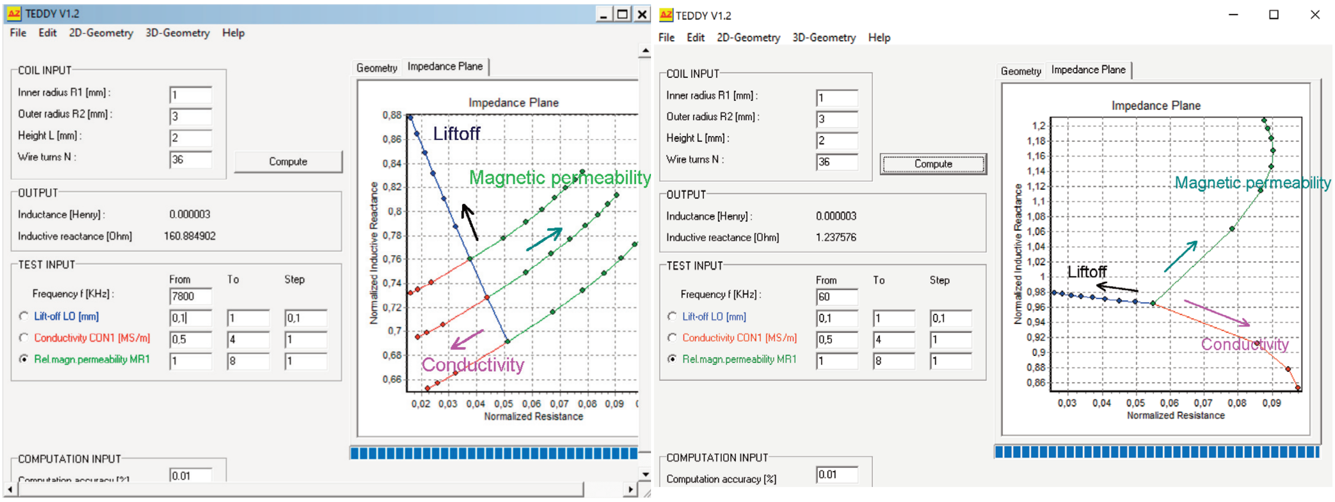

Simulation at $f = 7.8$ MHz Simulation at $f = 7.8$ MHz

Fig. 13. Simulations by TEDDY simulator [62].

3.5. Comparison of measurements against simulations

The EC measurement results can be compared to the Dodd–Deeds model (see [9] and further publications), for example, as implemented by Prof T. Theodoulidis [62] in the TEDDY software, which simulates the complex impedance of the measurement coil above a metal plate. An example of the simulation is given in Fig. 13. The parameters (geometry, number of turns, and impedance) are similar to those of coil P used in the experiments.

The X-axis shows the real component, and the Y-axis represents the imaginary component of the sensor coil impedance, normalized by the inductive apparent imaginary impedance XL0 in air. In the absence of metal in the proximity, the normalized impedance has a value of 1.00 (100%) for the imaginary component and 0.0 (0%) for the real component.

For $f = 7.8$ MHz (simulations at 7.6, 7.7, 7.8, and 7.9 MHz showed very similar results), the simulation demonstrates a similar behavior comparable to the experimental results. From the $f = 7.8$ MHz case (Fig. 13a), we observe the following:

- The impedance – in both real and imaginary components – is highly dependent on the liftoff.
- It is difficult to distinguish the impedance change resulting from the conductivity vs magnetic permeability of the specimen; they follow the same trend, but with opposite effects – an increase in conductivity leads to a decrease in permeability (and vice versa).
- However, the change in liftoff vs conductivity-permeability change is quite well distinguishable, as the lines are nearly orthogonal. This provides a basis for estimating liftoff variation from higher-frequency (e.g., 7.8 MHz) measurements, as shown in Fig. 13, making it feasible to apply a liftoff correction to the measured impedance of the sensor coil.

At much lower frequency, at $f = 60$ kHz (Fig. 13b), the magnetic permeability and electrical conductivity are quite well distinguishable from the complex plane of the sensor coil impedance, which is not the case at higher frequencies, e.g., in the 5 to 10 MHz range. Such separation of the electrical and magnetic properties of the OuT could be interesting for many other applications of NDT.

4. Conclusion and future work

In conclusion, the current work demonstrates that inductive (ECT) testing is a sensible and precise method for detecting even small defects. As expected, the experiments confirm that using higher frequencies (up to 10 MHz) enables clear and sensitive surface characterization. However, a multifrequency approach (e.g., combining a lower frequency on the order of 100 kHz with a higher frequency in the MHz range) is also beneficial for providing a more comprehensive characterization of both the surface and subsurface features of the saw blade material.

As for the specific conclusion concerning the detection of small (early-stage) cracks in the saw blade, a possible solution has been proposed. The approach is original, combining experimental investigation and model-based simulations, thereby providing a more reliable foundation than existing solutions. However, a key challenge remains: implementing this solution for high-speed, real-life measurements. Addressing this would push the current boundaries of the state of the art. The proposed model-based approach could be further empowered through the integration of machine learning techniques and by developing significantly improved (especially in terms of measurement speed) impedance measurement instrumentation.

Future work could include:

- Preparing a testbench for further real-time experiments, capable of working also at high speeds (testing between 10 000 and 100 000 saw blade teeth per second).
- Developing a corresponding simple but precise impedance measurement device, capable of measuring sensor coil impedance in the frequency range up to 10 MHz, with a resolution of at least 0.01% to 0.1% (thus requiring a

14- to 16-bit analogue front end), and performing at least several tens of thousands of measurements per second. The basis for such a device could be an FPGA-based small impedance measurement device [63] or the Digilent Analog Discovery 2 or 3 device, which provides a fully digital signal processing solution with a 14-bit analogue front end operating above 10 MHz.
- Instead of a black-box approach, applying a white-box approach to ECT, i.e., using analytical or numerical forward and inverse eddy current models.
- Investigating and testing image-based test systems, e.g., by using a line-scan camera (as suggested for high-speed coin validation [64]) and/or laser-line scanner principle [65].

Data availability statement

Data generated during this study are included in this article, the input data for analysis are available at https://github.com/omartens/eddy1.

Acknowledgments

This work was supported by the Estonian Research Council (grant No. PRG1483) and in part by the EU Horizon Europe research and innovation programme (5G-TIMBER project, grant agreement No. 101058505). The authors also thank Prof. T. Theodoulidis for his kind and long-standing support in eddy current simulation models. The publication costs of this article were partially covered by the Estonian Academy of Sciences.

References

1. Martens, O., Land, R., Metshein, M., Abdullayev, A., Vennikas, H. and Le Moullec, Y. Detection of cracks in a sawblade by eddy current measurements. In *2024 19th Biennial Baltic Electronics Conference (BEC), Tallinn, Estonia, 2–4 October 2024*. IEEE, 2024, 1–6.
2. Mordia, R. and Kumar Verma, A. Visual techniques for defects detection in steel products: a comparative study. *Eng. Fail. Anal.*, 2022, **134**, 106047. https://doi.org/10.1016/j.engfailanal.2022.106047
3. García-Martín, J., Gómez-Gil, J. and Vázquez-Sánchez, E. Non-destructive techniques based on eddy current testing. *Sensors (Basel)*, 2011, **11**(3), 2525–2565. https://doi.org/10.3390/s110302525
4. Machado, M. A. Eddy currents probe design for NDT applications: a review. *Sensors*, 2024, **24**(17), 5819. https://doi.org/10.3390/s24175819
5. Wikipedia. Eddy-current testing. https://en.wikipedia.org/wiki/Eddy-current_testing (accessed 2024-12-03).
6. Center for Nondestructive Evaluation. Depth of penetration and current density. https://www.nde-ed.org/Physics/Electricity/depthcurrentdensity.xhtml (accessed 2010-07-01).
7. Desjardins, D., Krause, T. W. and Clapham, L. Transient eddy current method for the characterization of magnetic permeability and conductivity. *NDT & E Int.*, 2016, **80**, 65–70. https://doi.org/10.1016/j.ndteint.2016.02.010
8. Nonaka, Y. A double coil method for simultaneously measuring the resistivity, permeability, and thickness of a moving metal sheet. *IEEE Trans. Instrum. Meas.*, 1996, **45**(2), 478–482. https://doi.org/10.1109/19.492771
9. Dodd, C. V. and Deeds, W. E. Analytical solutions to eddy-current probe-coil problems. *J. Appl. Phys.*, 1968, **39**(6), 2829–2838. https://doi.org/10.1063/1.1656680
10. Dodd, C. V. and Deeds, W. E. Absolute eddy-current measurement of electrical conductivity. Technical report. Oak Ridge National Lab, Tennessee, USA, 1981.
11. Burke, S. K. and Ibrahim, M. E. Mutual impedance of air-cored coils above a conducting plate. *J. Phys. D: Appl. Phys.*, 2004, **37**(13), 1857–1868. https://doi.org/10.1088/0022-3727/37/13/021
12. Zhang, J., Yuan, M., Xu, Z., Kim, H.-J. and Song, S.-J. Analytical approaches to eddy current nondestructive evaluation for stratified conductive structures. *J. Mech. Sci. Technol.*, 2015, **29**(10), 4159–4165. http://dx.doi.org/10.1007/s12206-015-0910-7
13. Theodoulidis, T. P., Tsiboukis, T. D. and Kriezis, E. E. Analytical solutions in eddy current testing of layered metals with continuous conductivity profiles. *IEEE Trans. Magn.*, 1995, **31**(3), 2254–2260. https://doi.org/10.1109/20.376236
14. Pokatilov, A., Parker, M., Kolyshkin, A., Märtens, O. and Kübarsepp, T. Inhomogeneity correction in calibration of electrical conductivity standards. *Measurement*, 2013, **46**(4), 1535–1540. https://doi.org/10.1016/j.measurement.2012.12.007
15. Reidla, M., Martens, O., Land, R. and Rist, M. Piccolo-stick and PCB-coil based simple coin validator. In *2012 5th European DSP Education and Research Conference (EDERC), Amsterdam, Netherlands, 13–14 September 2012*. IEEE, 2012, 81–84.
16. Howells, G. *Coin discriminators*. US Patent 7584833, 2009-09-08.
17. Märtens, O., Min, M., Land, R., Annus, P., Saar, T. and Reidla, M. *Method and device for frequency response measurement*. US Patent 88540302014, 2014-10-07.
18. Land, R., Annus, P., Min, M., Märtens, O. and Ojarand, J. *Method and device for broadband analysis of systems and substances*. US Patent 10698023, 2020-06-30.
19. Gordon, R. et al. Eddy current validation of Euro-coins. In *Lecture Notes on Impedance Spectroscopy: Measurement, Modeling and Applications 3* (Kanoun, O., ed.). CRC Press, London, 2012, 47–63.
20. Märtens, O., Land, R., Gordon, R., Min, M., Rist, M. and Pokatilov, A. Precise eddy current measurements: improving accuracy of determining of the electrical conductivity of metal plates. In *Lecture Notes on Impedance Spectroscopy: Measurement, Modeling and Applications 4* (Kanoun, O., ed.). Taylor & Francis, London, 2014, 109–115.
21. Märtens, O., Land, R., Min, M., Rist, M., Annus, P. and Pokatilov, A. Fast precise eddy current measurement of metals. In *2018 IEEE International Instrumentation and Measurement Technology Conference (I2MTC), Houston, USA, 14–17 May 2018*. IEEE, 2018, 1–5.
22. Märtens, O., Land, R., Min, M., Rist, M., Ferenets, M. and Käsper, A. Eddy current corrosion measurement of steel. In *Impedance Spectroscopy. Advanced Applications: Battery Research, Bioimpedance, System Design* (Kanoun, O., ed.). De Gruyter, Berlin, Boston, 2018, 125–134. https://doi.org/10.1515/9783110558920-012
23. He, Y., Tian, G., Zhang, H., Alamin, M., Simm, A. and Jackson, P. Steel corrosion characterization using pulsed eddy current systems. *IEEE Sens. J.*, 2012, **12**(6), 2113–2120. https://doi.org/10.1109/JSEN.2012.2184280
24. Laansoo, A., Kübarsepp, J., Surženkov, A., Land, R., Märtens, O. and Viljus, M. Induction brazing of cermets to steel and eddy current testing of joint quality. *Weld. World*, 2020, **64**, 563–571. https://doi.org/10.1007/s40194-020-00854-x
25. Kong, Y., Bennett, C. J. and Hyde, C. J. A review of non-destructive testing techniques for the in-situ investigation of fretting fatigue cracks. *Mater. Des.*, 2020, **196**, 109093. https://doi.org/10.1016/j.matdes.2020.109093
26. Torbali, M. E., Zolotas, A. and Avdelidis, N. P. A state-of-the-art review of non-destructive testing image fusion and critical

insights on the inspection of aerospace composites towards sustainable maintenance repair operations. *Applied Sciences*, **13**(4) 2023. https://doi.org/10.3390/app13042732
27. Silva, M. I., Malitckii, E., Santos, T. G. and Vilaca, P. Review of conventional and advanced non-destructive testing techniques for detection and characterization of small-scale defects. *Prog. Mater. Sci.*, 2023, **138**, 101155. https://doi.org/10.1016/j.pmatsci.2023.101155
28. Hutt, T. and Cawley, P. Feasibility of digital image correlation for detection of cracks at fastener holes. *NDT Int.,* 2009, **42**(2), 141–149. https://doi.org/10.1016/j.ndteint.2008.10.008
29. Marot, J., Bourennane, S. and Spinnler, K. Metal surface control system based on successive contour estimation. In *2010 IEEE International Conference on Image Processing*, *Hong Kong, China, 26–29 September 2010*. IEEE, 2010, 2293–2296.
30. Senthikumar, M., Palanisamy, V. and Jaya, J. Metal surface defect detection using iterative thresholding technique. In *Second International Conference on Current Trends In Engineering and Technology (ICCTET), Coimbatore, India, 8 July 2014*. IEEE, 2014, 561–564.
31. Hao, C., He, Y., Li, Y., Niu, X. and Wang, Y. An image-based hairline crack identification method for metal parts. *IEEE Trans. Instrum. Meas.*, 2023, **72**, 200114. https://doi.org/10.1109/TIM.2023.3324689
32. Zhang, Z., Wang, W. and Tian, X. Semantic segmentation of metal surface defects and corresponding strategies. *IEEE Trans. Instrum. Meas.*, 2023, **72**, 5016813. https://doi.org/10.1109/TIM.2023.3282301
33. Aslam, M., Khan, T. M., Naqvi, S. S., Holmes, G. and Naffa, R. On the application of automated machine vision for leather defect inspection and grading: a survey. *IEEE Access*, 2019, **7**, 176065–176086. https://doi.org/10.1109/ACCESS.2019.2957427
34. Tao, X., Gong, X., Zhang, X., Yan, S. and Adak, C. Deep learning for unsupervised anomaly localization in industrial images: a survey. *IEEE Trans. Instrum. Meas.*, 2022, **71**, 5018021. https://doi.org/10.1109/TIM.2022.3196436
35. Kumar, A. Computer-vision-based fabric defect detection: a survey. *IEEE Trans. Ind. Electron.*, 2008, **55**(1), 348–363. https://doi.org/10.1109/TIE.1930.896476
36. Luo, Q., Fang, X., Liu, L., Yang, C. and Sun, Y. Automated visual defect detection for flat steel surface: a survey. *IEEE Trans. Instrum. Meas.*, 2020, **69**(3), 626–644. https://doi.org/10.1109/TIM.2019.2963555
37. Agnisarman, S., Lopes, S., Chalil Madathil, K., Piratla, K. and Gramopadhye, A. A survey of automation-enabled human-in-the-loop systems for infrastructure visual inspection. *Autom. Constr.*, 2018, **97**, 52–76. https://doi.org/10.1016/j.autcon.2018.10.019
38. Ciampa, F., Mahmoodi, P., Pinto, F. and Meo, M. Recent advances in active infrared thermography for non-destructive testing of aerospace components. *Sensors*, 2018, **18**(2), 609. https://doi.org/10.3390/s18020609
39. He, Y., Li, M., Meng, Z., Chen, S., Huang, S., Hu, Y. et al. An overview of acoustic emission inspection and monitoring technology in the key components of renewable energy systems. *Mech. Syst. Signal Process.*, 2021, **148**, 107146. https://doi.org/10.1016/j.ymssp.2020.107146
40. Santos, S. D. and Furui, S. Quaternion signal processing for nonlinear ultrasonics. In *2024 19th Biennial Baltic Electronics Conference (BEC), Tallinn, Estonia, 2–4 October 2024*. IEEE, 2024, 1–6.
41. Foerster Group. *Non-Destructive Material Testing: The Most Important Methods for Crack Testing and Their Applications*. CT-0011 Rissprüfung ebook EN 223006, 2020.
42. Foerster Group. *Statograpgh CM+ / CM*. https://www.foerstergroup.com/en/products/statograph-cm-cm (accessed 2024-08-03).
43. USNR (Millwide). *BMS – Bandsaw Monitoring System*. https://www.usnr.com/en/product/bandsawmonitoringsystem (accessed 2024-12-03).
44. Lu, H. *Fatigue cracking of lumber bandsaw blades*. PhD thesis. University of British Columbia, Canada, 1993. http://dx.doi.org/10.14288/1.0081019
45. Tuck, D. L. Bandsaw diagnostics by neurocomputing-two are better than one! In *Proceedings 1995 Second New Zealand International Two-Stream Conference on Artificial Neural Networks and Expert Systems, Dunedin, New Zealand, 20–23 November 1995*. IEEE, 1995, 330–333.
46. Zhu, N., Tanaka, C. and Ohtani, T. Automatic detection of a damaged cutting tool during machining II: method to detect gullet crack in a bandsaw during sawing. *J. Wood Sci.*, 2001, **47**, 490–492. https: //doi.org/10.1007/BF00767903
47. Zhuo, R., Deng, Z., Chen, B., Liu, T., Ge, J., Liu, G. et al. Research on online intelligent monitoring system of band saw blade wear status based on multi-feature fusion of acoustic emission signals. *Int. J. Adv. Manuf. Technol.*, 2022, **121**, 4533–4548. https://doi.org/10.1007/s00170-022-09515-3
48. Auld, B. A. and Moulder, J. C. Review of advances in quantitative eddy current nondestructive evaluation. *J. Nondestruct. Eval.*, 1999, **18**, 3–36. https://doi.org/10.1023/A:1021898520626
49. Li, P., Xie, S., Wang, K., Zhao, Y., Zhang, L., Chen, Z. et al. A novel frequency-band-selecting pulsed eddy current testing method for the detection of a certain depth range of defects. *NDT Int.*, 2019, **107**, 102154. https://doi.org/10.1016/j.ndteint.2019.102154
50. Xie, S., Chen, Z., Takagi, T. and Uchimoto, T. Efficient numerical solver for simulation of pulsed eddy-current testing signals. *IEEE Trans. Magn.*, 2011, **47**(11), 4582–4591. https://doi.org/10.1109/TMAG.2011.2151872
51. Huang, P., Li, Z., Long, J., Xu, L. and Xie, Y. Measurement of lift-off distance and thickness of nonmagnetic metallic plate using pulsed eddy current testing. *IEEE Trans. Instrum. Meas.*, 2023, **72**, 6006810. https://doi.org/10.1109/TIM.2023.3285918
52. Chen, Z., Miya, K. and Kurokawa, M. Rapid prediction of eddy current testing signals using *A*–φ method and database. *NDT & E International*, 1999, **32**(1), 29–36. https://doi.org/10.1016/S0963-8695(98)00025-5
53. Skarlatos, A., Theodoulidis, T. and Poulakis, N. A fast and robust semi-analytical approach for the calculation of coil transient eddy-current response above planar specimens. *IEEE Trans. Magn.*, 2022, **58**(9), 6301609. https://doi.org/10.1109/TMAG.2022.3183019
54. Xia, Z., Huang, R., Chen, Z., Yu, K., Zhang, Z., Salas-Avila, J. R. et al. Eddy current measurement for planar structures. *Sensors*, 2022, **22**(22), 8695. https://doi.org/10.3390/s22228695
55. Silva, M. I., Malitckii, E., Santos, T. G. and Vilaça, P. Review of conventional and advanced non-destructive testing techniques for detection and characterization of small-scale defects. *Prog. Mater. Sci.*, 2023, **138**, 101155. https://doi.org/10.1016/j.pmatsci.2023.101155
56. Fukutomi, H., Huang, H., Takagi, T. and Tani, J. Identification of crack depths from eddy current testing signal. *IEEE Trans. Magn.*, 1998, **34**(5), 2893–2896. https://doi.org/10.1109/20.717674
57. Mirshekar-Syahkal, D. and Mostafavi, R. F. 1-D probe array for ACFM inspection of large metal plates. *IEEE Trans. Instrum. Meas.*, 2002, **51**(2), 374–382. https://doi.org/10.1109/19.997840
58. Chen, G.-M., Li, W. and Wang, Z. Structural optimization of 2-D array probe for alternating current field measurement. *NDT Int.*, 2007, **40**(6), 455–461. https://doi.org/10.1016/j.ndteint.2007.03.002
59. Karpenko, O., Efremov, A., Ye, C. and Udpa, L. Multi-frequency fusion algorithm for detection of defects under fasteners with EC-GMR probe data. *NDT Int.*, 2020, **110**, 102227. https://doi.org/10.1016/j.ndteint.2020.102227

60. Martens, O. Precise synchronous detectors with improved dynamic reserve. *IEEE Trans. Instrum. Meas.*, 2002, **49**(5), 1046–1049. https://doi.org/10.1109/19.872928
61. Texas Instruments. *LDC Reference Coils User's Guide*. Literature No. SNOU136, 2015.
62. Theodoulidis, T. and Kotouzas, M. Eddy current testing simulation on a personal computer. In *15th World Conference on Nondestructive Testing, Roma, Italy, 15–21 October 2000*. AIPnD, 2000.
63. Priidel, E., Pesti, K., Min, M., Ojarand, J. and Märtens, O. FPGA-based 16-bit 20 MHz device for the inductive measurement of electrical bio-impedance. In *2021 IEEE International Instrumentation and Measurement Technology Conference (I2MTC)„ Glasgow, UK, 17–20 May 2021*. IEEE, 2021, 1–6.
64. Gavrijaseva, A., Märtens, O., Land, R. and Reidla, M. Coin recognition using line scan camera. In *2014 14th Biennial Baltic Electronic Conference (BEC), Tallinn, Estonia, 6–8 October* 2014. IEEE, 2014, 161–164.
65. Molder, A., Martens, O., Saar, T. and Land, R. Adaptively undersampled image processing for fast multiline laser detection. In *2013 IEEE 8th International Symposium on Intelligent Signal Processing, Funchal, Portugal, 16–18 September 2013*. IEEE, 2013, 60–64.

Metallide pinnadefektide tuvastamine: juhtumiuuring

Olev Märtens, Raul Land, Margus Metshein, Anar Abdullayev, Henri Vennikas, Yannick Le Moullec ja Marek Rist

Metallpindade defekte saab tuvastada mitmel viisil. Üks võimalus on visuaalne kontroll. Teine lihtne ja tõhus meetod on pöörisvoolu testimine (ECT). Metallide, nende sulamite ja struktuuride pöörisvoolul (magnetinduktsioonil) põhinevat mõõtmist saab kasutada nii nende mittepurustavaks testiks kui ka metallide (sh erinevate klasside, nt teraste) tuvastamiseks, paksuse mõõtmiseks, katete omaduste hindamiseks, korrodeerunud (ka värvikihi all) alade leidmiseks ning termilise või muu töötlemise kvaliteedi iseloomustamiseks. Impedantsspektroskoopia võimaldab ühe mõõtmisega määrata mitmeid metallide omadusi ja saada teavet ka materjali või struktuuri sügavusprofiili kohta. Reaalajas tootmises on võimalikud kiired ja täpsed mõõtmised (nt kuni 100 mõõtmist sekundis). Näiteks puidutöötlemistööstuses on üks oluline protsess materjali lõikamine lintsaega, mille lõikekiirus ületab 50 m/s. Ohutuse, kvaliteedi ja hoolduse seisukohalt on kasulik varakult tuvastada saehammaste läheduses tekkivaid pragusid.

Kuigi on olemas ka teisi meetodeid, nagu akustilise emissiooni või vibratsiooni mõõtmine protsessi käigus, on elektromagnetiline (enamasti pöörisvoolupõhine) testimine levinuim lähenemisviis. Töös antakse ülevaade olemasolevatest testimislahendustest. Samuti käsitletakse ühe mõranenud saelehe proovi uurimist pöörisvoolu mõõtmise teel, kasutades sagedusvahemikus 100 kHz–10 MHz erinevaid tasapinnalisi (trükkplaadi) pooli. Katsetulemused näitavad, et meetod toimib tõhusalt. Kõrgemad mõõtmissagedused annavad ootuspäraselt parema ülevaate pinnapragude tekkest. Suurim probleem on mikropragude väiksuse tõttu nende tuvastamine. Töö tulemused näitavad ka, et edasised uuringud peaksid keskenduma mõõtmise kiiruse suurendamisele ja pragude kiirele tuvastamisele (nt kuni 100 000 saehamba testimine sekundis). Esitatakse ka mitmeid soovitusi võimalike lähenemisviiside kohta ning käsitletakse lühidalt masinnägemisel põhinevaid võimalusi.